Elsevier Editorial System(tm) for
Construction & Building Materials
Manuscript Draft

Manuscript Number: CONBUILDMAT-D-17-02179R1

Title: Stabilization and solidification of a heavy metal contaminated site soil using a hydroxyapatite based binder

Article Type: Research Paper

Keywords: Heavy metal contaminated soil; hydroxyapatite; strength; leachability; solidification and stabilization.

Corresponding Author: Professor YanJun Du, PhD

Corresponding Author's Institution: Southeast University

First Author: WeiYi Xia , PhD

Order of Authors: WeiYi Xia , PhD; YaSong Feng , PhD; Fei Jin, PhD; LiMing Zhang, Master; YanJun Du, PhD

Abstract: Synthetic hydroxyapatite (HA) is an efficient and environment-friendly material for the remediation of heavy metal contaminated soils. However, the application of conventional HA powder in stabilizing contaminated soils is limited, due to high cost of final products, difficulties in synthesizing purified HA crystals. A new binder named SPC, which composes of single superphosphate (SSP) and calcium oxide (CaO), is presented as an alternative in this study. HA can form in the soil matrix by an acid-base reaction between SSP and CaO, resulting in a dense structure and improved mechanical properties of treated soils. Therefore, the SPC is capable of effectively immobilizing heavy metals and elevating strength of contaminated soils, meanwhile, maintaining relatively low cost. This paper presents a systematic investigation of the performance, reaction products, and microstructural properties of a lead (Pb), zinc (Zn), and cadmium (Cd) contaminated industrial site soil stabilized with SPC binder. The effects of SPC content and curing time on the pH, leachability and strength properties of the stabilized soils are evaluated. Furthermore, modified European Communities Bureau of Reference (BCR) sequential extraction procedure (SEP), mercury intrusion porosimetry (MIP), X-ray diffraction (XRD), and scanning electron microscope (SEM) analyses are performed to interpret the mechanisms controlling the changes in these macro-properties. The results show that the soil pH and unconfined compressive strength (UCS) increase with increasing SPC content and curing time. After 28 days of curing, the UCS values of stabilized soils are approximately 2.2 to 5.7 times those of the untreated soil. The leachability of Pb, Zn and Cd is significantly reduced after stabilization, and the SPC content and curing time have considerable influences on the leached concentrations of heavy metals. The SEP results confirm that SPC significantly reduces the acid soluble fractions of Pb, Zn and Cd while increases their residual fractions. The MIP test results show that pore volume reduces notably and pore profile of the soil changes remarkably after SPC stabilization. The mineralogical (XRD) and microstructural (SEM) analyses reveal that the formation of heavy metal-bearing hydroxyapatites and phosphate-based precipitates are

the primary mechanisms of immobilization of Pb, Zn and Cd in the SPC stabilized soil.

Research Highlights

- SPC significantly improves strength and reduces leachability of the soils
- SPC effectively reduces volume and size of inter-aggregate and air pores
- SPC stabilization significantly reduces acid soluble fractions of heavy metals
- Hydroxyapatite and heavy metal-bearing hydroxyapatite form in stabilized soils

Figure 1

Click here to download high resolution image

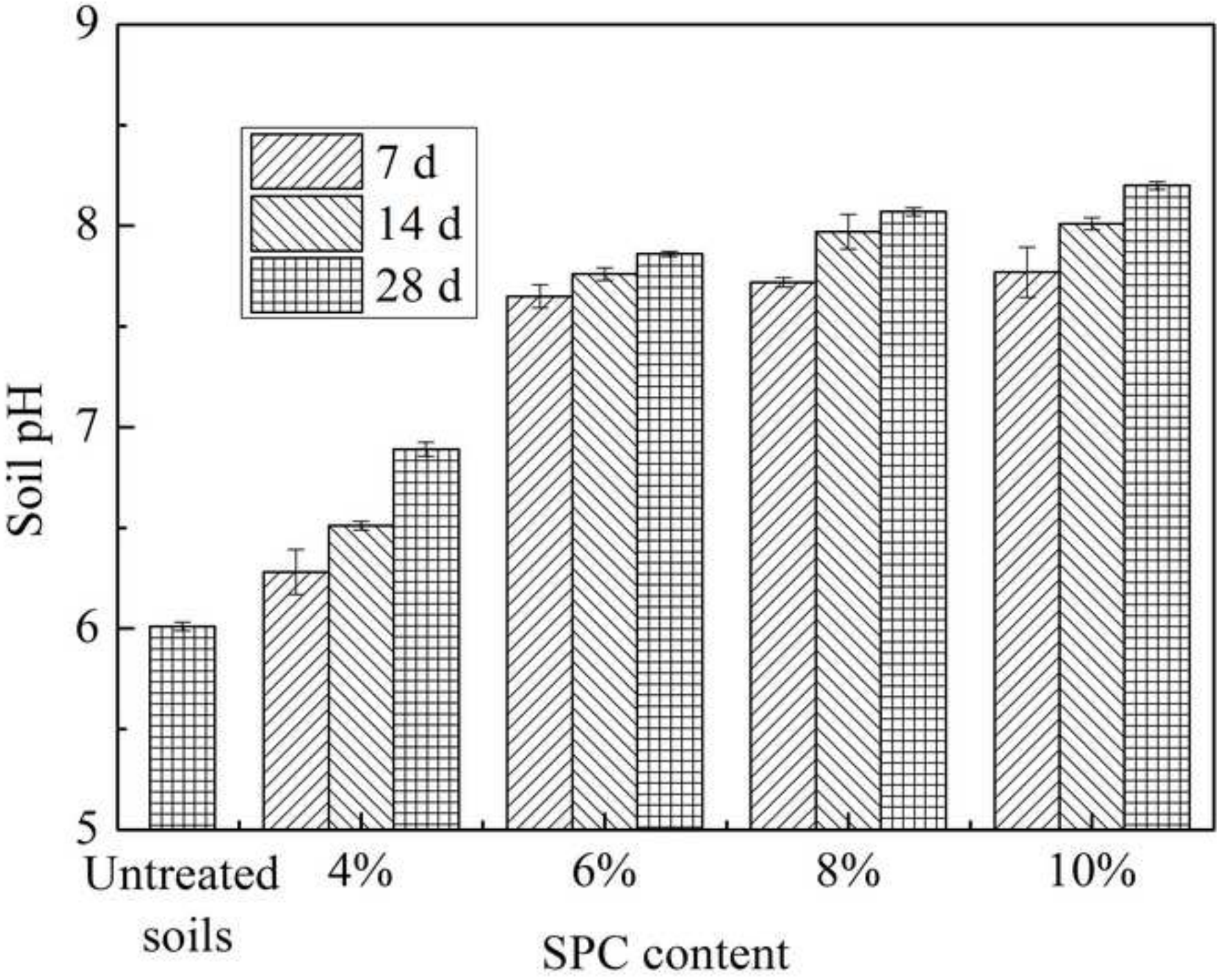

Figure 2

Click here to download high resolution image

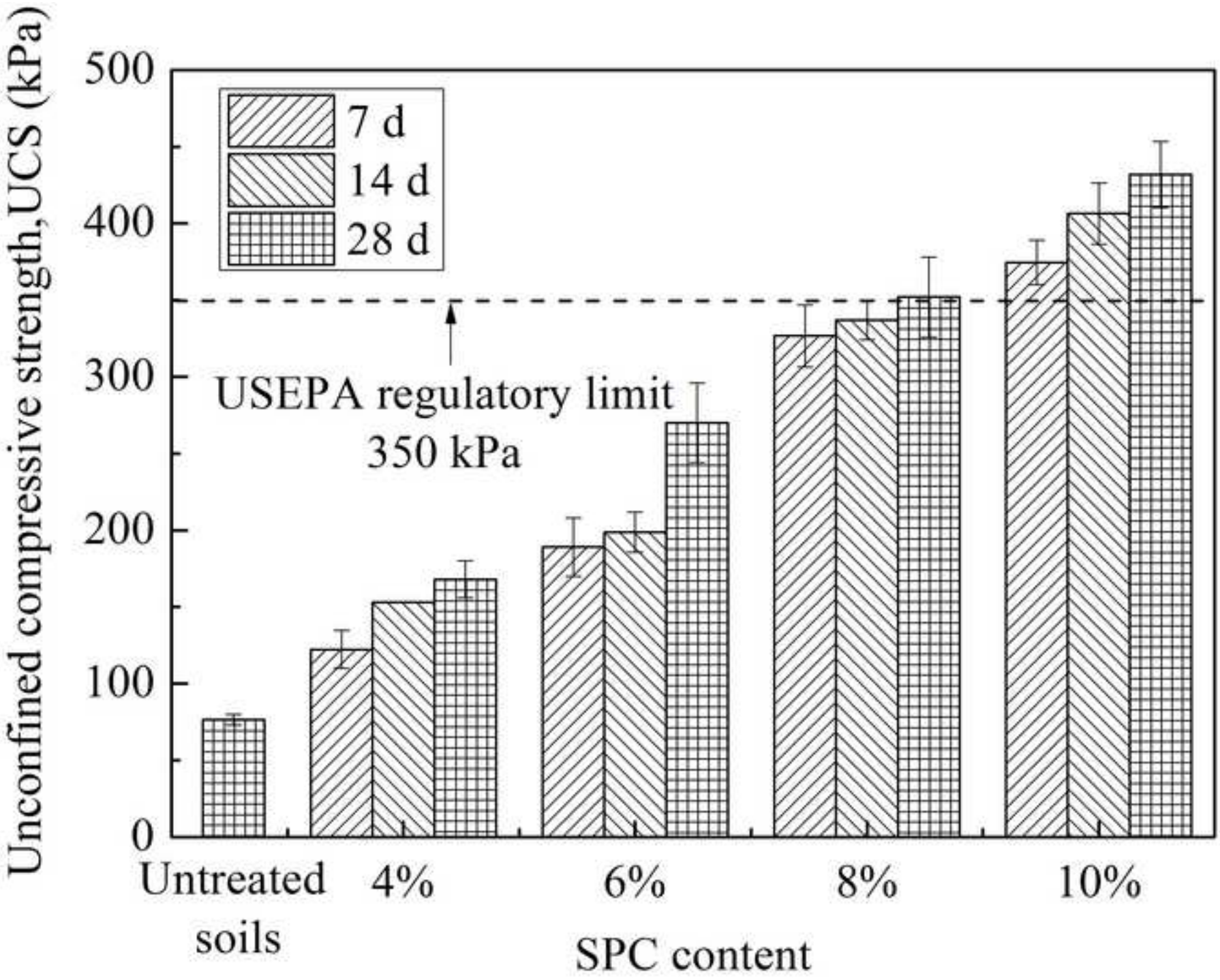

Figure 3(a)
Click here to download high resolution image

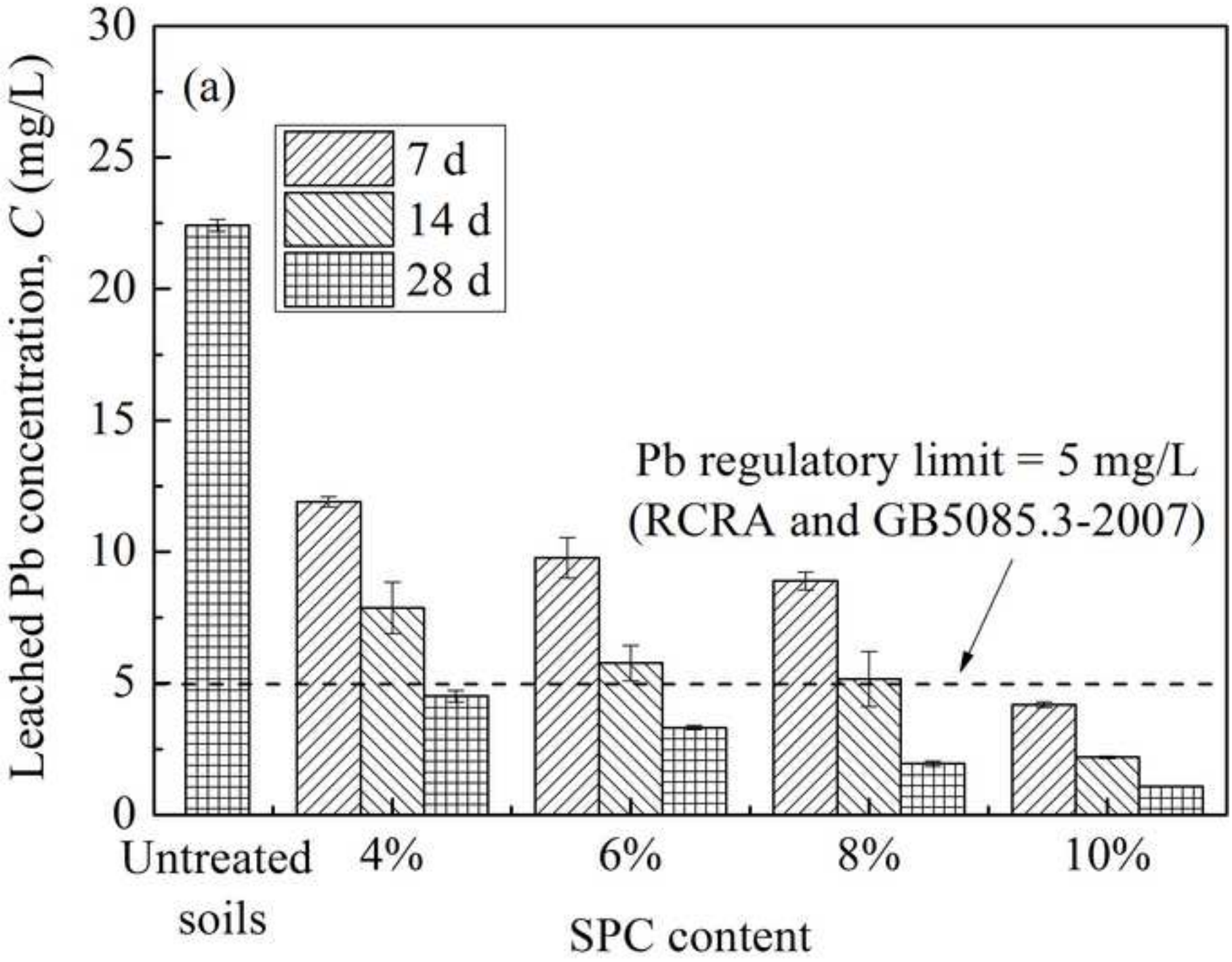

Figure 3(b)
Click here to download high resolution image

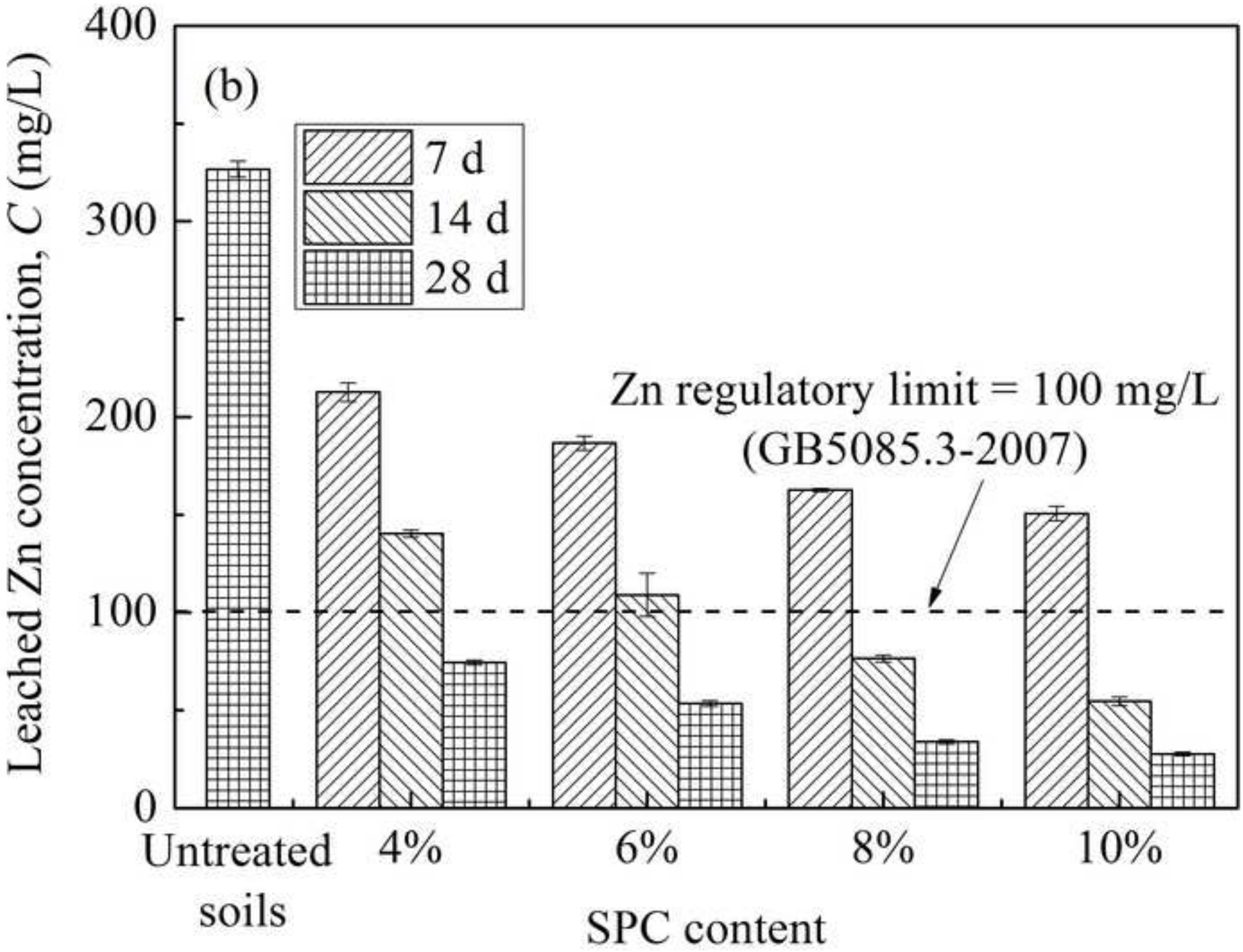

Figure 3(c)
Click here to download high resolution image

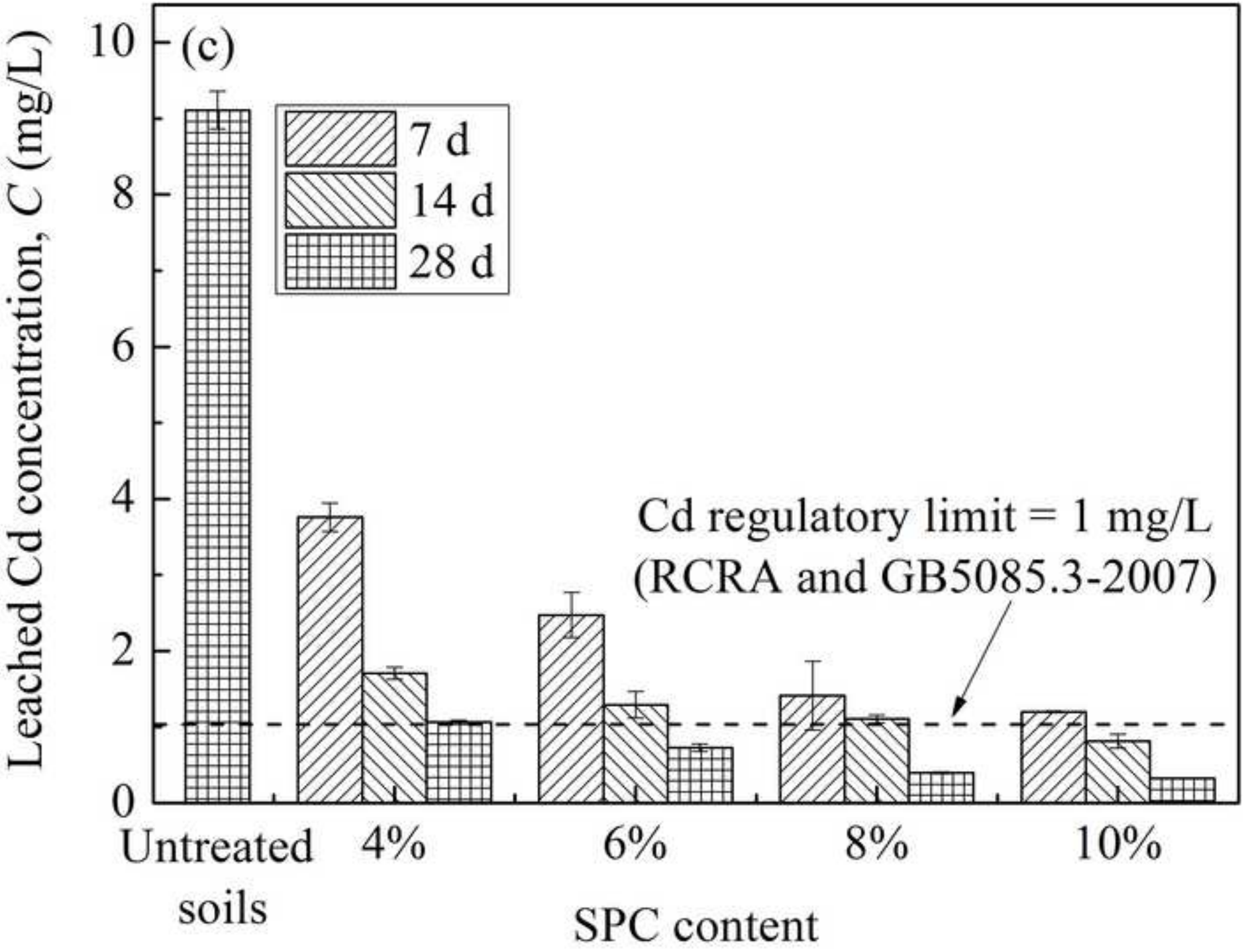

Figure 4

Click here to download high resolution image

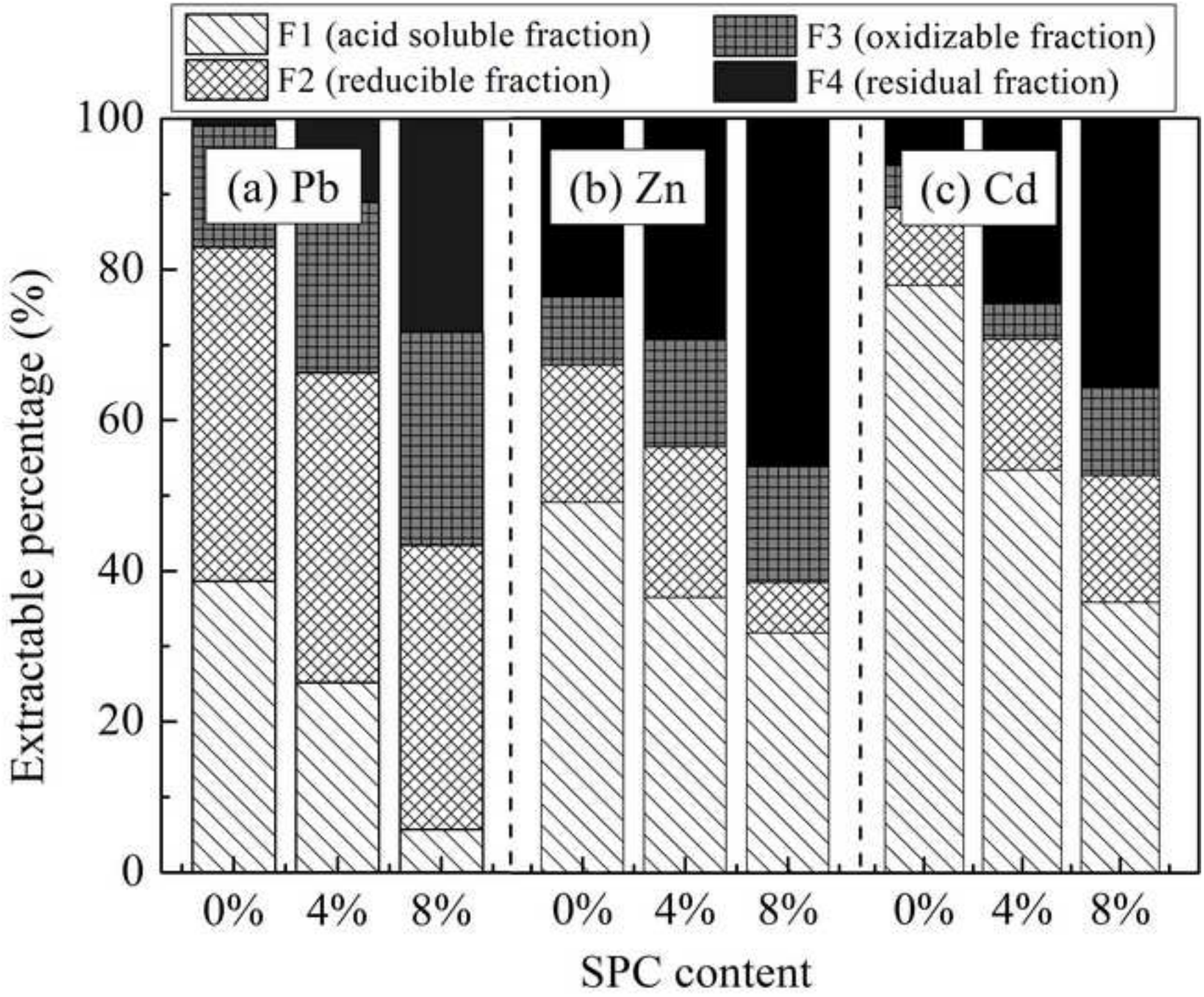

Figure 5(a)
Click here to download high resolution image

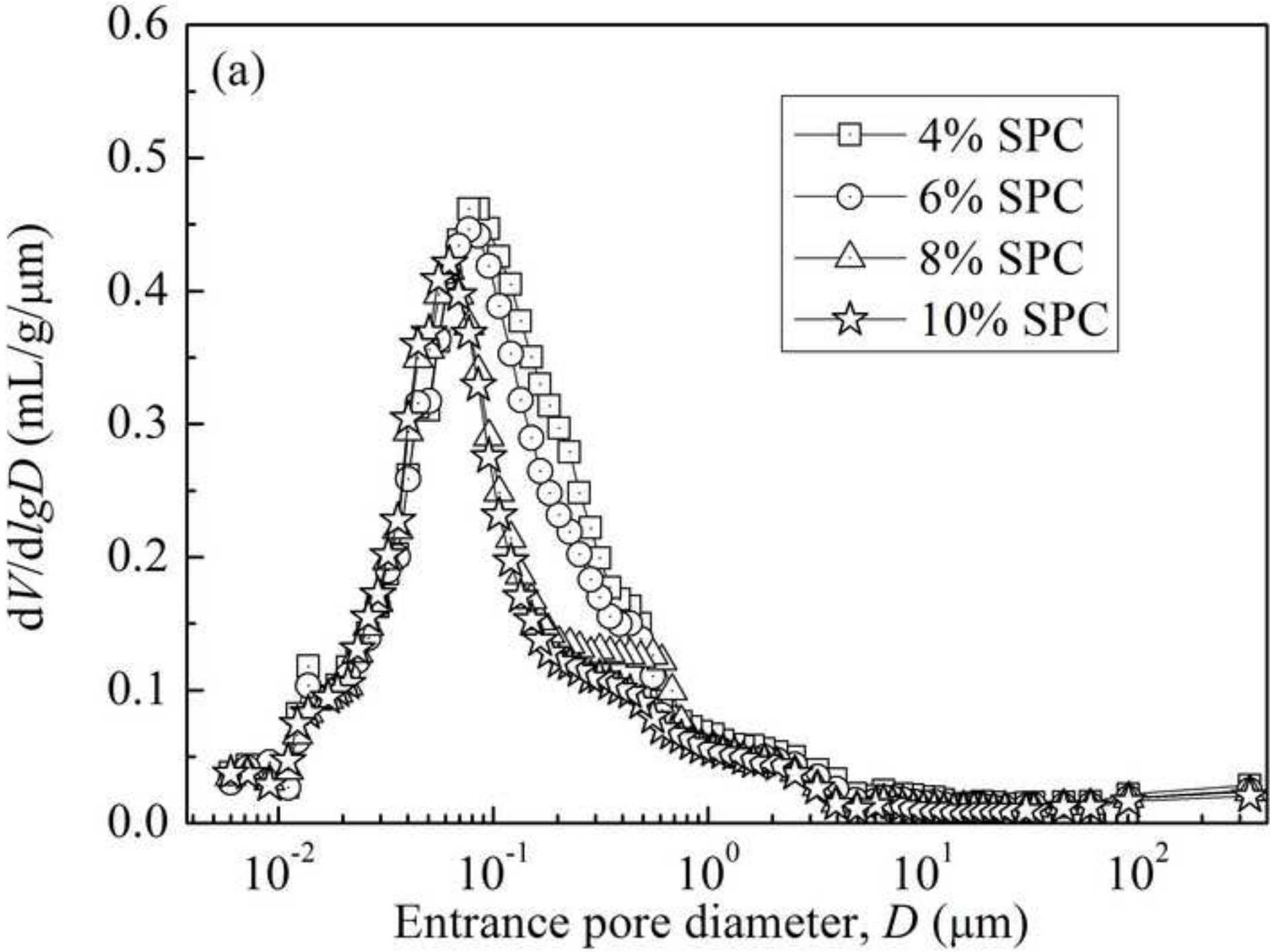

Figure 5(b)
Click here to download high resolution image

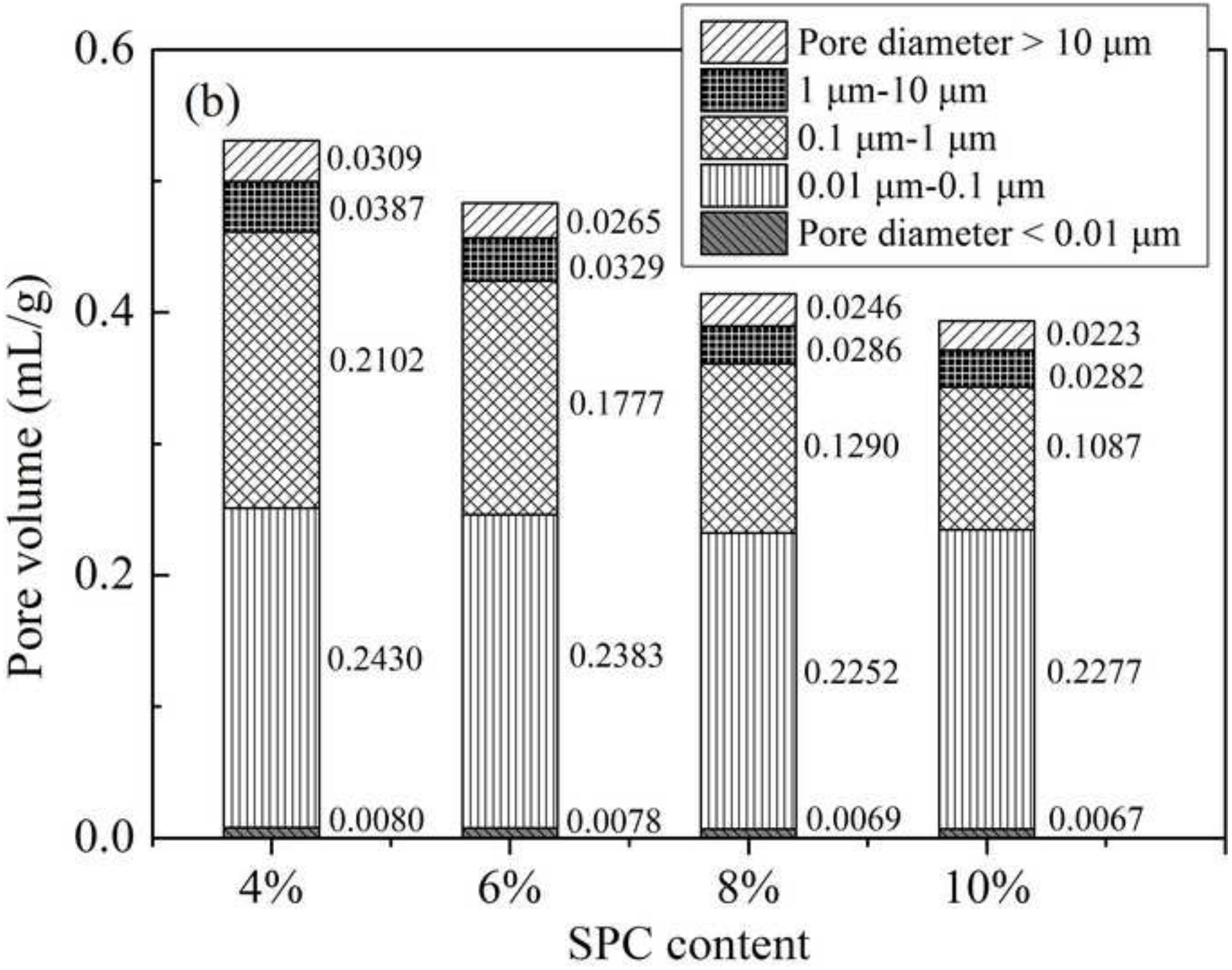

Figure 6

Click here to download high resolution image

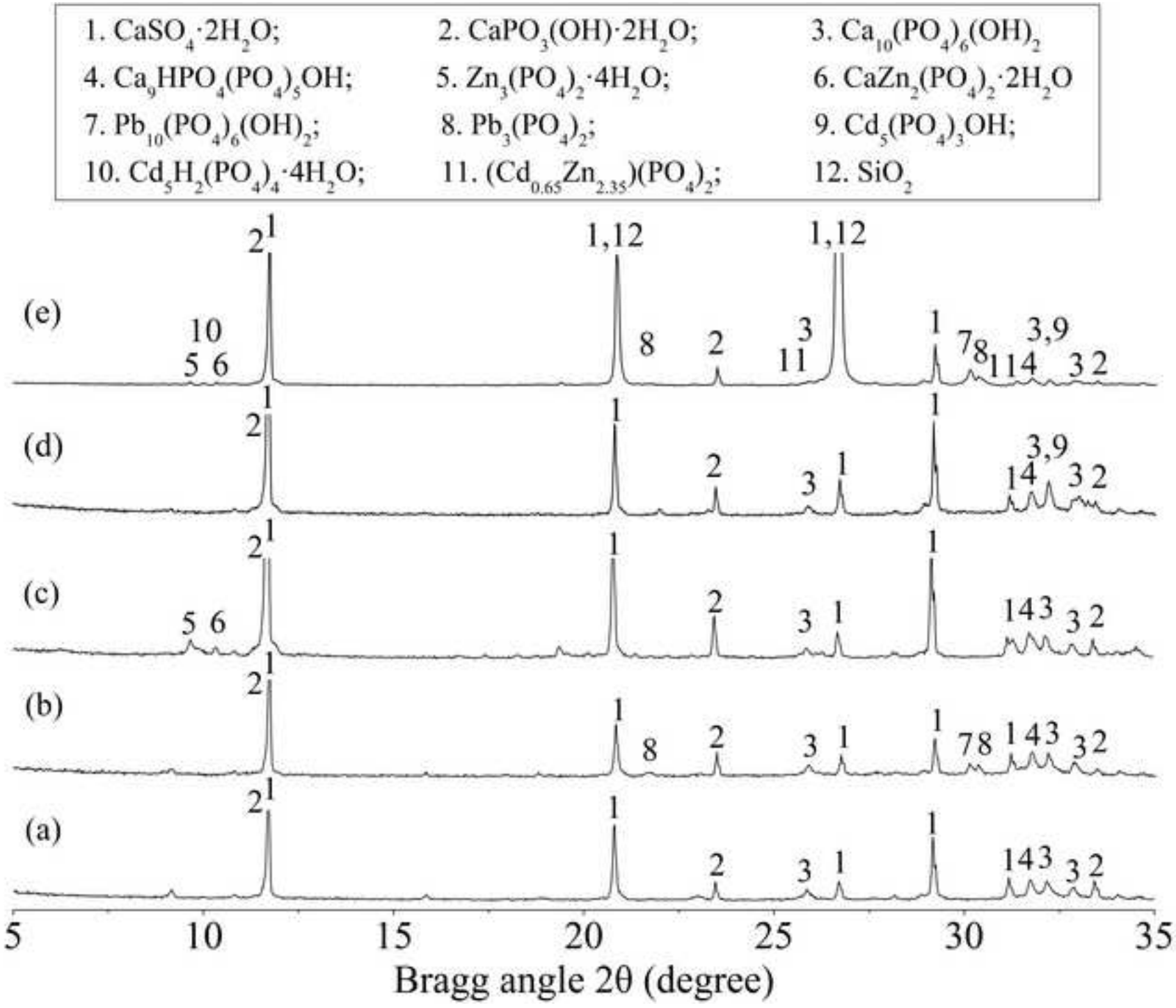

Figure 7

Click here to download Figure: Figure 7.pdf

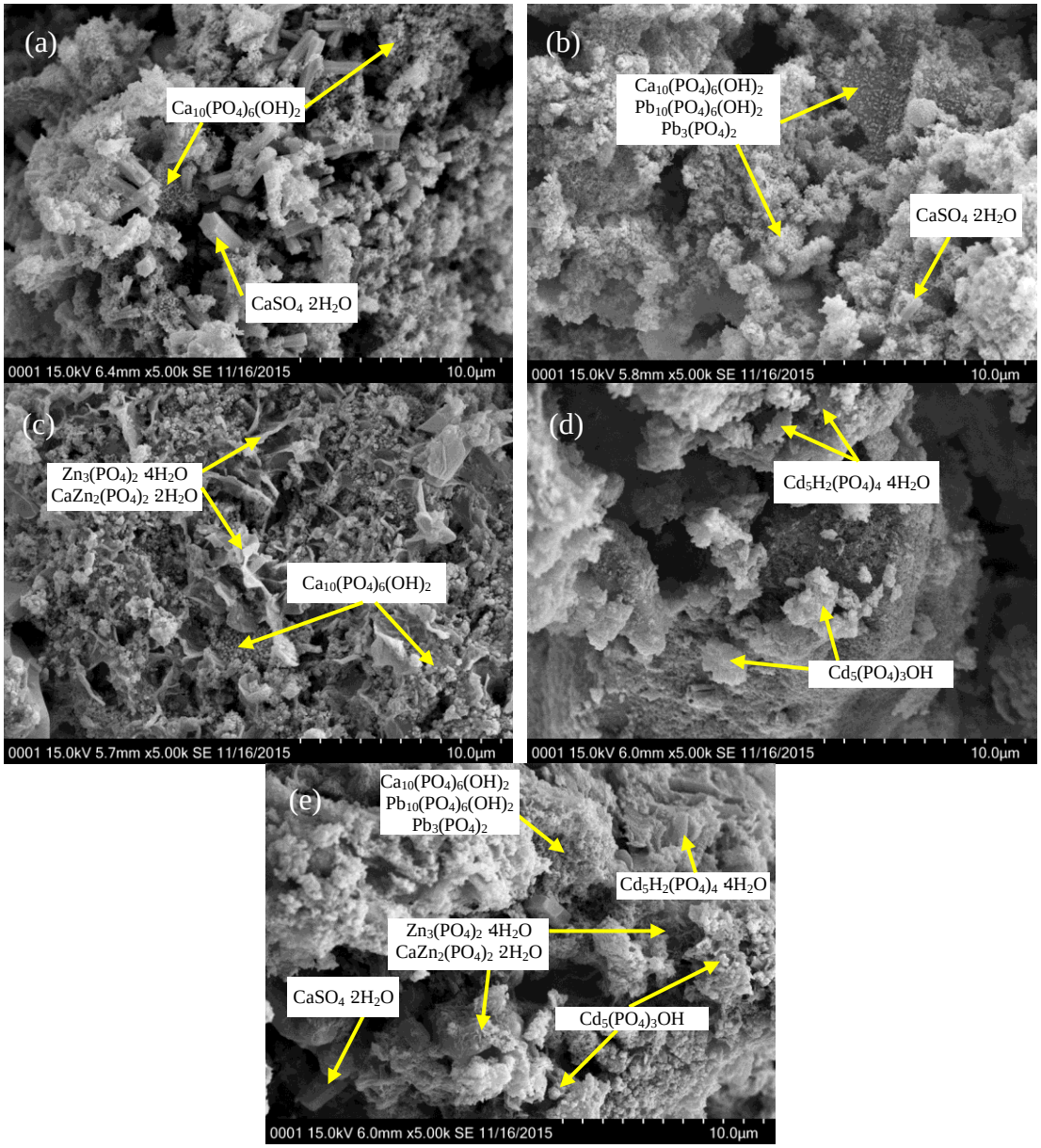

Stabilization and solidification of a heavy metal contaminated site soil using a hydroxyapatite based binder

Wei-Yi Xia, Ya-Song Feng, Fei Jin, Li-Ming Zhang, Yan-Jun Du*

Wei-Yi Xia
PhD Student, Jiangsu Key Laboratory of Urban Underground Engineering & Environmental Safety, Institute of Geotechnical Engineering, Southeast University, Nanjing 210096, China. Email: diguosj@163.com

Ya-Song Feng
PhD Student, Jiangsu Key Laboratory of Urban Underground Engineering & Environmental Safety, Institute of Geotechnical Engineering, Southeast University, Nanjing 210096, China. Email: fengyasongys@126.com

Fei Jin
Research associate, Department of Engineering, University of Cambridge, Trumpington Road, Cambridge CB2 1PZ, United Kingdom. E-mail: leonking1987@gmail.com

Li-Ming Zhang
Graduate Student, Jiangsu Key Laboratory of Urban Underground Engineering & Environmental Safety, Institute of Geotechnical Engineering, Southeast University, Nanjing 210096, China. Email: z13951925373@163.com

Yan-Jun Du*
Professor, Jiangsu Key Laboratory of Urban Underground Engineering & Environmental Safety, Institute of Geotechnical Engineering, Southeast University, Nanjing 210096, China (*Corresponding author). Tel: +86-25-83793729, Fax: +86-25-83795086. Email: duyanjun@seu.edu.cn

Technical Paper Submitted for Possible Publication in

Construction and Building Materials

Abstract: Synthetic hydroxyapatite (HA) is an efficient and environment-friendly material for the remediation of heavy metal contaminated soils. However, the application of conventional HA powder in stabilizing contaminated soils is limited, due to high cost of final products, difficulties in synthesizing purified HA crystals. A new binder named SPC, which composes of single superphosphate (SSP) and calcium oxide (CaO), is presented as an alternative in this study. HA can form in the soil matrix by an acid-base reaction between SSP and CaO, resulting in a dense structure and improved mechanical properties of treated soils. Therefore, the SPC is capable of effectively immobilizing heavy metals and elevating strength of contaminated soils, meanwhile, maintaining relatively low cost. This paper presents a systematic investigation of the performance, reaction products, and microstructural properties of a lead (Pb), zinc (Zn), and cadmium (Cd) contaminated industrial site soil stabilized with SPC binder. The effects of SPC content and curing time on the pH, leachability and strength properties of the stabilized soils are evaluated. Furthermore, modified European Communities Bureau of Reference (BCR) sequential extraction procedure (SEP), mercury intrusion porosimetry (MIP), X-ray diffraction (XRD), and scanning electron microscope (SEM) analyses are performed to interpret the mechanisms controlling the changes in these macro-properties. The results show that the soil pH and unconfined compressive strength (UCS) increase with increasing SPC content and curing time. After 28 days of curing, the UCS values of stabilized soils are approximately 2.2 to 5.7 times those of the untreated soil. The leachability of Pb, Zn and Cd is significantly reduced after stabilization, and the SPC content and curing time have considerable influences on the leached concentrations of heavy metals. The SEP results confirm that SPC significantly reduces the acid soluble fractions of Pb, Zn and Cd while increases their residual fractions. The MIP test results show that pore volume reduces notably and pore profile of the soil changes remarkably after SPC stabilization. The mineralogical (XRD) and microstructural

(SEM) analyses reveal that the formation of heavy metal-bearing hydroxyapatites and phosphate-based precipitates are the primary mechanisms of immobilization of Pb, Zn and Cd in the SPC stabilized soil.

Key words: Heavy metal contaminated soil; hydroxyapatite; strength; leachability; solidification and stabilization.

1 Introduction

In China, the accumulation of contaminations including heavy metals and organic compounds and other hazardous pollutants in industrial site soils during the last two decades is of increasing concern due to the potential health risks [1]-[3]. According to the "Report on the National General Survey on Soil Contamination" published in 2014 [4], 36.3% of heavily-polluted industrial sites, 34.9% of abandoned industrial sites, and 33.4% of mining sites in China are contaminated by heavy metals, particularly lead (Pb), zinc (Zn) and cadmium (Cd). 7% of surveyed sites exhibit high total concentrations of Cd. Moreover, Pb and Zn are also found in large quantities in 1.5% and 0.9% of surveyed sites, respectively. There is an urgent need to develop cost-effective methods to remediate Pb, Zn and Cd contaminated site soils.

Stabilization/solidification (S/S), the addition of lime, cement and other cementitious binders to soils or wastes to fix and encapsulate contaminants, has been considered the "best demonstrated available technology (BDAT)" to treat most toxic contaminants [5]. In recent years, sustainable binders such as geopolymers using fly ash, slag and cement kiln dust have been successfully used in pavement engineering applications [6],[7]. As the most stable calcium phosphate salt at ambient temperature and pH between 4 and 12 [8], hydroxyapatite ($Ca_{10}(PO_4)_6(OH)_2$, HA, $K_{sp} = 2.35\times10^{-59}$) has an excellent ion-exchangeability and is an efficient material to capture heavy metals [9],[10]. It is reported that synthetic HA powder can effectively immobilize heavy metals and therefore enhance their geochemical stability in contaminated soils [11].

The immobilization of Pb, Zn and Cd by HA is mainly attributed to two mechanisms: (1) rapid surface adsorption and complexation on surface available adsorption sites of the HA [12] , which are primarily responsible for Zn and Cd immobilization, while approximately 30% of Pb is immobilized by the surface adsorption or complexation as reported by

Mavropoulos et al. [13], and (2) the formation of stable and insoluble heavy metal-bearing HA ($(Ca_{10-x}M_x)(PO_4)_6(OH)_2$) (M = Pb, Zn or Cd, $0 \leq x \leq 10$) [14] and phosphate-based precipitates including parascholzite ($CaZn_2(PO_4)_2 \cdot 2H_2O$, $K_{sp} = 10^{-34.1}$) and hopeite ($Zn_3(PO_4)_2 \cdot 4H_2O$, $K_{sp} = 1.2 \times 10^{-17}$), through cation exchange reactions where Pb, Zn and Cd replace calcium (Ca) on HA lattices, which is controlled by HA dissolution rate and predominates the Pb immobilization [15],[16].

Conventional applications of HA in treating contaminated soils are usually conducted by mixing HA powder with soils [17],[18]. However, the methods to synthesize HA powder with desired characteristics including wet synthesis, soli-state reaction and hydrothermal processes, have several disadvantages. For instance, they usually require complicated experiment operations, controlled working temperatures, and expensive equipments and therefore result in high-cost of final products (~ $20,000/ton) [19],[20].

Instead of pre-preparation of HA powder, this study presents a new low-cost powder binder SPC (~ $120/ton) to immobilize Pb, Zn, and Cd and improve the mechanical properties of contaminated soils in the meantime. The SPC composes of single superphosphate (SSP) and calcium oxide (CaO) powders with a dry weight ratio of 1:3. SSP is a quick-acting phosphate fertilizer extensively used in agriculture, and manufactured by the reaction between sulfuric acid (H_2SO_4) and raw phosphate rock ($Ca_5(PO_4)_3F$, $K_{sp} = 10^{-55.71}$). Hence SSP is a mixture of monocalcium phosphate ($Ca(H_2PO_4)_2 \cdot H_2O$, solubility = 1.9 g/100 mL) and calcium sulfate ($CaSO_4$, $K_{sp} = 9.1 \times 10^{-6}$). It is reported that a self-setting calcium phosphate cement can be prepared by mixing $Ca(H_2PO_4)_2 \cdot H_2O$ and CaO [21]. This calcium phosphate cement has HA as its main final product, and has been proven to be a very efficient bone substitute in different applications [22]. According to Wang et al. [23], $Ca(H_2PO_4)_2 \cdot H_2O$ can react with CaO to yield HA ($Ca_{10}(PO_4)_6(OH)_2$) as expressed by the following equation:

$$3Ca(H_2PO_4)_2 \cdot H_2O + 7CaO \rightarrow Ca_{10}(PO_4)_6(OH)_2 + 8H_2O \quad (1)$$

114 It is hypothesized that the Pb, Zn and Cd immobilization with SPC in contaminated soils
115 may involve two mechanisms: (1) in the presence of soil pore water, phosphate ions (PO_4^{3-},
116 $HPO_4^{2-}$and $H_2PO_4^-$) can be released from $Ca(H_2PO_4)_2 \cdot H_2O$ and react with Pb, Zn and Cd to
117 form metal phosphate precipitates such as lead phosphate ($Pb_3(PO_4)_2$, $K_{sp} = 10^{-44.6}$),
118 $Zn_3(PO_4)_2 \cdot 4H_2O$ and pentacadmium dihydrogen tetrakis (phosphate) tetrahydrate
119 ($Cd_5H_2(PO_4)_4 \cdot 4H_2O$, $K_{sp} = 10^{-30.9}$), respectively [24],[25], and (2) the immobilization of
120 heavy metals by HA, which includes surface adsorption, complexation, formation of heavy
121 metal-bearing hydroxyapatites and metal phosphates precipitates, via substitution of Ca in
122 HA by metals [15],[16].

123 The objective of this paper is to assess the feasibility of utilizing the novel binder SPC to
124 stabilize a Pb, Zn, and Cd contaminated industrial site soil. Analyses are conducted with
125 respect to the effects of SPC content and curing time on the performance characteristics of
126 stabilized soils including soil pH, strength, and heavy metals leachability. Additionally,
127 modified European Communities Bureau of Reference (BCR) sequential extraction procedure
128 (SEP), X-ray diffraction (XRD), scanning electron microscope (SEM), and mercury intrusion
129 porosimetry (MIP) analyses are carried out to explore the immobilization mechanisms of Pb,
130 Zn, and Cd by SPC and study the pore size distributions of the stabilized soils, which are
131 essential for interpreting the changes in leachability and strength properties. The results of
132 this study will provide useful information and facilitate the use of SPC binder for stabilizing
133 heavy metal contaminated soils.

134

135 **2 Materials and methods**

136 **2.1 Materials**

137 The soil tested is collected from a Pb–Zn smelter contaminated site (36° 33’ N, 104° 12’
138 E) located in a suburb area of the northeast Baiyin City, Gansu Province of China. As one of

the largest smelters in the northwest of China, this smelter has been operated continually since 1996, and has a severe impact on the local environment. Each year, the smelter produces approximately 130000 tons of Zn, 50000 tons of Pb, and 365 tons of Cd. The intensive industrial activities of metal smelting in the past two decades have yield elevated heavy metal contaminations in soils with a depth of approximately 3.0 m surrounding the smelter. Surface soil with a depth of approximately 0.5 m is sampled, placing in polyethylene bags, and transported to the laboratory.

Before use, the soil is air-dried, screened (≤ 1 mm) and thoroughly homogenized. The physicochemical properties of the soil are shown in **Table 1**. It can be found that this contaminated site soil exhibits extremely high total concentrations of Pb (9710 mg/kg), Zn (17300 mg/kg) and Cd (2425 mg/kg). In addition, the organic matter content of the soil tested is found to be 3.19%. The SPC composes of 75% SSP and 25% CaO powders (dry weight basis). The SSP (chemically pure) and CaO (analytical reagent) are obtained from Sinopharm Chemical Reagent Co. Ltd. and Nanjing Chemical Reagent Co. Ltd. respectively. The main chemical compositions of SSP and CaO are shown in **Table 2**.

2.2 Sample preparation

Before use, both SSP and CaO are crushed and ground to pass through a sieve with 0.075 mm mesh. In this study, the SPC contents are set as 0% (i.e. untreated soil), 4%, 6%, 8% and 10% (dry weight basis). The stabilized soil samples are prepared via the following procedure. Firstly, deionized water is poured into the sieved soil until water content reaches 22% (i.e., optimum water content of the untreated soil). The soil and water are thoroughly mixed with a bench-top electric agitator to create a homogeneous mixture. The water content herein is defined as the ratio of the weight of the water to that of total solids including oven-dried soil (95 °C for 24 h) and binder. Secondly, the predetermined weights of SSP and

CaO powders are added together to the soil-water mixture and the mixture is mixed thoroughly for about 6 minutes to achieve homogeneity. The mixture is then poured into a cylindrical mold with diameter of 50 mm and height of 100 mm in five layers [29] and statically compacted by a hydraulic jack to achieve a dry density of 1.51×10^3 kg/m^3, which is the same with the maximum dry density of the untreated soil. Finally, the soil is carefully extruded from the mold using a hydraulic jack, wrapped by a polythene bag to avoid loss of water, and subjected to standard curing condition (95% relative humidity and 22 °C) for 7, 14, and 28 days. The compaction method is used to prepare soil samples to simulate a field scenario where the treated soils are used as roadway subgrade materials.

Divalent metals e.g., Pb, Zn, and Cd, have similar geochemical and environmental properties [30]. The association of Pb, Zn, and Cd in the soils and their chemical similarity can lead to interaction among them and the change of reaction products during S/S by SPC. It is important to investigate the effect of co-existing metals on the immobilization mechanisms through an analysis of differences in products formed in SPC solidified matrix containing single metal and ternary metals. Therefore, the SPC pastes spiked with Pb, Zn, and Cd are prepared for XRD and SEM tests to understand the interactions between heavy metals and SPC binder. To prepare pastes containing 3% metal, $Pb(NO_3)_2$, $Zn(NO_3)_2\cdot6H_2O$ and $Cd(NO_3)_2\cdot4H_2O$ (analytical reagents) solutions are added into the SPC powder to obtain Pb, Zn, and Cd contents of 30000 mg/kg (dry weight basis). Selecting metal nitrates as sources to spike the SPC pastes is because that nitrate ion is chemically inert as compared with chloride, sulfate, and acetate ions, to react with the main chemical compositions including Ca and PO_4 in SPC binder [1],[31]. Predetermined volume of deionized water is then poured into the powder to obtain slurry with a water-binder ratio of 2.97:1, which is the same with the water-binder ratio of the 8% SPC stabilized soil. The slurry is stirred up for about 6 minutes using an electric mixer to achieve homogeneity. The mixture is then filled in three layers

189 inside the cylindrical PVC mold with 50 mm in diameter and 100 mm in height, and the PVC
190 mold is immediately wrapped by polythene film and cured with the temperature of 22 °C and
191 relative humidity of 95%. After 28 days of curing, the paste samples are carefully extracted
192 from the mold and subjected to XRD and SEM analyses.

193 Three identical samples are prepared for soil pH, unconfined compressive strength
194 (UCS), and toxicity characteristic leaching procedure (TCLP) tests, and one sample is used
195 for the analyses of SEP, MIP, XRD, and SEM, respectively. The mean values of the triplicates
196 subjected to soil pH, TCLP and UCS tests are given in **Figs. 1** to **3** (error bars represent
197 standard deviations). The SPC contents and curing time of samples subjected to various tests
198 are listed in **Table 3**.

199

200 **2.3 Testing methods**

201 The UCS tests as per ASTM D4219 [32] with a fixed strain rate of 1%/min are conducted
202 on all of the stabilized and untreated soils samples at designated curing times. A certain
203 quantity of the fresh soil is sampled carefully from the broken UCS specimen and is then
204 subjected to pH, TCLP and SEP tests. Meanwhile, approximately 1 cm^3 subsamples are
205 carefully preserved and immediately frozen in nitrogen slush cooled at -195 °C, followed by
206 sublimation of the frozen water at -80 °C in a vacuum desiccator. These freeze-dried samples
207 are then subjected to MIP, XRD and SEM analyses.

208 The pH of the untreated and stabilized soils is measured by employing HORIBA pH
209 METER D-54 as per ASTM D492 [33]. Leachability of heavy metals is evaluated using the
210 TCLP-EPA Method 1311 [34]. The initial pH of the TCLP extraction liquid (5.7 mL of
211 CH_3COOH and 64.3 mL of 1mol/L NaOH) is 4.93 ± 0.05.

212 The modified BCR four-step SEP is carried out to determine the chemical speciation of
213 heavy metals. The modified SEP test includes four individual extraction steps [35]: (1) acid

soluble fraction (F1), extraction in 0.11 mol/L CH_3COOH with pH of 2.8; (2) reducible fraction (F2), extraction in 0.5 mol/L $NH_2OH{\cdot}HCl$ with pH of 1.5; (3) oxidizable fraction (F3), oxidation in acid-stabilise 30% H_2O_2 and extraction in 1 mol/L CH_3COONH_4, both with pH of 2; and (4) residual fraction (F4), complete digestion using an acid mixture of HF, HNO_3, $HClO_4$ and H_2O_2. The F1 fraction contains the metals that are precipitated or co-precipitated with carbonate, is considered to be the most bioavailable metal forms. The F2 fraction is bound to iron (Fe) and manganese (Mn) oxides, which can be mobilized when environmental conditions become increasingly reducing. The F3 fraction is incorporated into stable organic matter and sulphides, which can be released under oxidizing conditions and is not considered mobile and bioavailable. The F4 fraction is tightly bound to the crystal lattices of minerals and inside crystallized oxides and is the most difficult fraction to remove, so this is assumed to remain in the soil for long periods. The mobility and bioavailability of heavy metals decrease approximately in the order of the extraction sequence [31].

The MIP test is carried out on an AutoPore IV 9510 mercury intrusion porosimeter with a maximum intrusion pressure of 413 MPa. The pore diameter intruded by mercury under an applied pressure, *P*, can be calculated by using the capillary pressure equation as following [29],[36] :

$$d = -\frac{4\tau\cos\alpha}{p} \tag{2}$$

where d (μm) is pore entry diameter; τ (N/m) is the surface tension of the mercury (4.84×10^{-4} N/mm at 25 °C in this study); α (°) and p (MPa) are contact angle and absolute applied pressure respectively (135° and 413 MPa in this study, respectively).

The freeze-dried samples are ground and sieved through a 0.075 mm sieve before XRD test. XRD is performed on 8% SPC stabilized soil, clean SPC paste and SPC pastes spiked with 3% Pb, Zn or Cd alone using a Rigaku D/Max-2500 X-ray diffractometer. Samples are

scanned from 5° to 70° with Cu-Kα (λ = 1.540538 Å) radiation and a scanning rate of 2°/min. The SEM analysis is conducted on the gold-coated samples using a LEO1530VP scanning electron with low accelerating voltage of 15 kV.

3 Results and analysis

3.1 Soil pH

Fig. 1 displays the variation of soil pH with SPC content at different curing times. It can be seen that the untreated soil is slightly acidic with a mean pH of 6.01, and the SPC treatment raises the soil pH with high SPC content resulting in high alkalinity. For instance, at 28 days, the pH values of 6%, 8% and 10% SPC stabilized samples are 7.86, 8.07 and 8.20 respectively, which are slightly alkaline while 4% SPC stabilized soil shows a nearly neutral pH of 6.89. In addition, for all stabilized soil samples tested, the pH values increase marginally with curing time.

3.2 Unconfined compression test

Fig. 2 shows the variation of UCS with SPC content at various curing time. Similar to the pH variation, the UCS of stabilized soils increases with increasing SPC content or curing time. In general, the most significant strength development is observed at the beginning 7 days and tends to be stabilized in the long term. As compared to curing time, the SPC content apparently has a more significant impact on the UCS development. For instance, at 28 days, the mean UCS values of 4% (168 kPa) and 6% (270 kPa) SPC stabilized samples are 2.2 and 3.5 times those of untreated samples, and the mean UCS values of 8% (352 kPa) and 10% (432 kPa) SPC stabilized samples are 4.7 and 5.7 times those of untreated samples, respectively. It is obvious that both 8% and 10% SPC stabilized samples cured for 28 days display higher UCS values than 350 kPa, which is recommended by the USEPA for the

stabilized materials to be disposed in a landfill [37].

3.3 TCLP test

Fig. 3 shows that the average leached Pb, Zn and Cd concentrations of untreated samples are 22.41, 326.71 and 9.11 mg/L respectively, suggesting their high mobility in the untreated soil. Leached metal concentrations for all stabilized samples are noticeably decreased after SPC treatment. In addition, increasing SPC content and curing time both are found to significantly reduce the Pb, Zn and Cd leachability. At 28 days, 4% SPC is able to reduce leachable Pb to below 5 mg/L, which is the toxicity characteristic (TC) limit specified by the Resource Conservation and Recovery Act (RCRA) and Chinese government standard of identification for extraction toxicity (GB 5085.3-2007). Increasing the SPC content to 10% achieves the goal after only 7 days of curing. Additions of 4% to 10% SPC result in leachable Zn concentrations of 74.55 to 27.71 mg/L, which are below the regulatory limit of GB 5085.3-2007 (100 mg/L). In the case of Cd, it generally requires 28 days to achieve the RCRA and GB 5085.3-2007 TC limit (1 mg/L) at SPC contents from 4% to 8%, while 10% SPC needs 14 days of curing. It can be concluded that the SPC stabilization can significantly immobilize Pb, Zn and Cd in the contaminated soil, thereby decreasing their leachability and potential toxicity.

3.4 Modified BCR SEP test

Fig. 4 shows the metal chemical speciation in the stabilized samples cured for 28 days measured by the modified BCR SEP test. For the untreated soil, the F1 fractions account for 38.61%, 49.13% and 77.88% of the total Pb, Zn and Cd respectively. Meanwhile, the F4 fractions are only 0.92%, 23.58% and 6.21% of the total Pb, Zn and Cd respectively. SPC is found to significantly reduce the F1 fractions and increase the F4 fractions. The F1 fractions

of Pb, Zn, and Cd in the 4% SPC stabilized soil are 25.16%, 36.50% and 53.36%, respectively, which are 34.82%, 25.71% and 31.49% lower than those of the untreated soil sample respectively. Increasing the SPC content reduces the F1 fractions. In the 8% SPC stabilized soil, the F1 fractions of Pb, Zn and Cd are only 5.68%, 31.79% and 35.86%. Similarly, the F4 fractions of Pb (28.25%), Zn (46.08%) and Cd (35.66%) in the 8% SPC stabilized soil are 2.6, 1.6 and 1.5 times those of the 4% SPC stabilized soil (11.06%, 29.30% and 24.53%, respectively), and 30.8, 2.0 and 5.7 times those of the untreated soil respectively. These results indicate that the SPC stabilized soils exhibit higher chemical stability of Pb, Zn and Cd as compared to the untreated contaminated soil.

3.5 Pore size distribution

Fig. 5(a) shows the pore size distributions (PSDs) of stabilized soils with different SPC contents. The *y*-axis is plotted as $f(D)$ ($f(D) = \mathrm{d}V/\mathrm{d}lgD$), where V is the volume of pores having a diameter of D in 1 g of the dry soil. The parameter $\mathrm{d}V/\mathrm{d}lgD$ is used because the area under the curve between any two pore diameters represents the volume of pores that are distributed between these two diameters [1],[38]. Bimodal PSDs are frequently observed in structured soils, and the peaks associated with larger and smaller diameters represent inter-aggregate and intra-aggregate pores respectively [39]. However, for all SPC stabilized soil samples in this study, the distributions are unimodal, with a prominent peak at ~0.100, 0.090, 0.071 and 0.065 μm in samples stabilized with 4%, 6%, 8% and 10% SPC respectively. In addition, the increase in SPC content significantly reduces the pore volume corresponding to the peak.

The volumes of different types of pores are shown in **Fig. 5(b)**. As suggested by Horpibulsuk et al. [36],[38], 0.01 and 10 μm are the thresholds between intra-aggregate and inter-aggregate pores, and inter-aggregate and air pores, respectively. In addition, according

to the pore diameters, inter-aggregate pores can be further subdivided into three subdivisions: 0.01 μm - 0.1 μm, 0.1 μm - 1 μm and 1 μm - 10 μm [36]. It is observed that when the SPC content increases from 4% to 10%, the total pore volume decreases steadily from 0.53 to 0.39 mL/g for stabilized soil samples. The volumes of inter-aggregate and air pores, especially the inter-aggregate pores between 0.1 μm to 1 μm decrease significantly with increasing SPC content. It is also observed that reduction of inter-aggregate pores primarily contributes to the reduction in the total pore volume. In addition, it is found that as the SPC content increases, the volume of intra-aggregate pores changes slightly. Previous studies [36],[38],[40] report that the inter-aggregate and air pores have remarkable effects on the strength properties of soils, as a result, the soil samples stabilized with higher content of SPC have superior mechanical performances than those stabilized with lower content of SPC.

3.6 X-ray diffraction analysis

The XRD results for the SPC paste, SPC pastes with 3% metals (Pb, Zn or Cd) and 8% SPC stabilized soil sample are presented in **Fig. 6**. In each of the diffractograms, the predominant minerals detected are gypsum ($CaSO_4 \cdot 2H_2O$, $K_{sp} = 4.93\times10^{-5}$), brushite ($CaPO_3(OH) \cdot 2H_2O$, $K_{sp} = 2.7\times10^{-7}$), HA ($Ca_{10}(PO_4)_6(OH)_2$) and calcium-deficient HA ($Ca_9HPO_4(PO_4)_5OH$, $K_{sp} = 10^{-85.1}$), having the primary reflection at 2θ of 11.63°, 11.60°, 31.77° and 31.72°, respectively. It is confirmed that a certain quantity of desired HA is formed in both the stabilized soil and SPC pastes. In addition, the SPC stabilized soil sample also shows peaks of quartz (SiO_2). The formations of $Zn_3(PO_4)_2 \cdot 4H_2O$ (2θ of 9.65°) and $CaZn_2(PO_4)_2 \cdot 2H_2O$ (2θ of 10.34°) are identified in both the SPC stabilized contaminated soil and SPC paste containing 3% Zn. Moreover, in both the 8% SPC stabilized soil and SPC paste containing 3% Pb, the major peaks of hydroxypyromorphite ($Pb_{10}(PO_4)_6(OH)_2$, $K_{sp} = 10^{-76.8}$, 2θ of 30.10°) and $Pb_3(PO_4)_2$ (2θ of 30.33°) are clearly recognizable. In the stabilized

soil, cadmium hydroxyapatite ($Cd_5(PO_4)_3OH$, K_{sp} = $10^{-64.62}$, 2θ of 32.20°), $Cd_5H_2(PO_4)_4 \cdot 4H_2O$ (2θ of 10.01°) and cadmium zinc phosphate ($(Cd_{0.65}Zn_{2.35})(PO_4)_2$, 2θ of 31.14°) are the detectable Cd-bearing phases. In the SPC paste containing 3% Cd, however, the primary peak reflections of $Cd_5H_2(PO_4)_4 \cdot 4H_2O$ and $(Cd_{0.65}Zn_{2.35})(PO_4)_2$ do not match the measured diffractograms, whereas the presence of $Cd_5(PO_4)_3OH$ is easily identified.

Although stabilized soil and SPC pastes have the same Pb and Zn-bearing products, considerable difference in formation of the Cd-bearing products is found. This indicates that coexistence of Pb, Zn, and Cd in the stabilized soil can induce the formation of new metal-minerals including $Cd_5H_2(PO_4)_4 \cdot 4H_2O$ and $(Cd_{0.65}Zn_{2.35})(PO_4)_2$. It is thought that the formation of $Cd_5H_2(PO_4)_4 \cdot 4H_2O$ in the stabilized soil is attributed to the influence of soil pH condition. The 8% SPC stabilized soil subjected to XRD analysis has a mean pH value of 8.07 (see **Fig. 1**). As suggested by Matusik et al. [25], the solution pH condition strongly affects the speciation of phosphate ions including PO_4^{3-}, HPO_4^{2-}, $H_2PO_4^{-}$, which in turn could alter the chemical composition of Cd-bearing precipitates resulting from the reactions between Cd and phosphate ions. The experimental results of aqueous Cd immobilization by addition of phosphates [25] demonstrate that $Cd_5H_2(PO_4)_4 \cdot 4H_2O$ crystals are formed at a solution pH lower than 8.50, but the increase of solution pH is adverse for the formation and crystallization of $Cd_5H_2(PO_4)_4 \cdot 4H_2O$. When solution pH is higher than 8.50, the formation of $Cd_5H_2(PO_4)_4 \cdot 4H_2O$ could not be detected. The pH value of the SPC paste containing 3% Cd tested in this study is 9.23, which is higher than the threshold value of 8.50 reported by Matusik et al. [25]. Therefore, formation of $Cd_5H_2(PO_4)_4 \cdot 4H_2O$ is detected in the 8% SPC stabilized soil but not in the SPC paste containing 3% Cd. The formation of $(Cd_{0.65}Zn_{2.35})(PO_4)_2$ in the 8% SPC stabilized soil is attributed to the ion-exchanges, in which the Zn or Cd presented in $Zn_3(PO_4)_2 \cdot 4H_2O$ and $CaZn_2(PO_4)_2 \cdot 2H_2O$ lattices is replaced by Cd.

3.7 Scanning electron microscope (SEM) analysis

The microstructures of the SPC paste, SPC pastes containing 3% metals (Pb, Zn or Cd) and 8% SPC stabilized soil examined by SEM are shown in **Fig. 7**. The needle-shaped and prismatic-shaped products in **Fig. 7(a)** represent HA ($Ca_{10}(PO_4)_6(OH)_2$) and $CaSO_4 \cdot 2H_2O$ in SPC paste, respectively, as reported by earlier researchers [41],[42]. From **Fig. 7(b)**, it can be observed that when Pb is present in the SPC paste, the morphology of $Ca_{10}(PO_4)_6(OH)_2$, $Pb_{10}(PO_4)_6(OH)_2$ or $Pb_3(PO_4)_2$ is well developed and the quantity is relatively large [43],[44]. When Zn is present in the SPC paste, as shown in **Fig. 7(c)**, it is observed that massive plate-like products including $Zn_3(PO_4)_2 \cdot 4H_2O$ and $CaZn_2(PO_4)_2 \cdot 2H_2O$ as well as needle-shaped $Ca_{10}(PO_4)_6(OH)_2$ precipitate on the surface of the SPC paste [45]. Presence of large quantities of cluster product of $Cd_5(PO_4)_3OH$ and amorphous $Cd_5H_2(PO_4)_4 \cdot 4H_2O$ have been observed in the SPC paste containing 3% Cd (see **Fig. 7 (d)**) [46],[47]. For the soil stabilized with 8% SPC, shown in **Fig. 7 (e)**, it is evident the surface of the soil grain is covered by large number of plate-like ($Zn_3(PO_4)_2 \cdot 4H_2O$ or $CaZn_2(PO_4)_2 \cdot 2H_2O$), cluster ($Cd_5(PO_4)_3OH$), amorphous ($Cd_5H_2(PO_4)_4 \cdot 4H_2O$), needle-shaped ($Ca_{10}(PO_4)_6(OH)_2$, $Pb_{10}(PO_4)_6(OH)_2$ or $Pb_3(PO_4)_2$) and prismatic-shaped ($CaSO_4 \cdot 2H_2O$) products [24],[47] that are identified by the XRD analysis.

4 Discussion

The SPC stabilized soils display higher pH as compared to the untreated soil. As the curing time and SPC content increase, the soil pH value increases (see **Fig. 1**). This observation is attributed to the formation of HA, which is a weak-alkaline compound (pH = 7 to 9) [48],[49], as substantiated from the XRD and SEM analyses.

It is seen from **Fig. 2** that the addition of SPC binder to the contaminated soil results in a notable increase in UCS. The strength increase of SPC stabilized soils can be attributed to the

following reasons: (1) the formation of calcium-phosphate crystals (HA, $CaPO_3(OH)\cdot 2H_2O$ and $Ca_9HPO_4(PO_4)_5OH$) that possess high chemical bonding strength and consequently creates cementation bonds between soil particles [49], and (2) the formation of various reaction products including HA, $CaSO_4\cdot 2H_2O$, $CaPO_3(OH)\cdot 2H_2O$ and $Ca_9HPO_4(PO_4)_5OH$ results in a denser structure of the SPC stabilized soil. This is substantiated by the MIP analysis (see **Fig. 5**) which shows that these minerals formed can fill the pores especially inter-aggregate pores (see **Fig. 5**). A small decrease in total pore volume is proved to be enough to generate a significant gain in strength, due to the existence of a larger number of contacts between soil particles [51],[52].

As seen in **Fig. 3**, the addition of SPC, even in the smallest amount of 4%, greatly reduces the metal leachability. This is attributed to that: (1) higher pH of stabilized soil samples (**Fig. 1**) which leads to their stronger resistance against acid attack as compared to untreated soil [53], and (2) reduced proportion of acid soluble metal fraction and higher proportion of residual fraction in the soil stabilized with higher SPC content (**Fig. 4**). The acid soluble fraction is sensitive to pH change and could be mobilized when the pH is lowered [54],[55]. After stabilization with SPC, the Pb, Zn, and Cd in soluble fractions can form heavy metal-bearing hydroxyapatites ($Pb_{10}(PO_4)_6(OH)_2$, $Cd_5(PO_4)_3OH$)) and phosphate-based precipitates including $Zn_3(PO_4)_2\cdot 4H_2O$, $CaZn_2(PO_4)_2\cdot 2H_2O$, $Pb_3(PO_4)$, $Cd_5H_2(PO_4)_4\cdot 4H_2O$ and $(Cd_{0.65}Zn_{2.35})(PO_4)_2$, as substantiated from the XRD patterns and SEM images (**Figs. 6** and **7**). These mineral phases are highly insoluble and tightly bound the metals to their crystal lattices, which explains the increase of the residue fractions of the heavy metals in the SEP tests.

As expected, the results and discussion above confirm that the SPC stabilization technology is a cost-effective method to immobilize Pb, Zn and Cd in the contaminated site soil. Furthermore, it has been reported that HA is effective in immobilizing other toxic metals

413 including copper (Cu), cobalt (Co), nickel (Ni) and antimony (Sb) [56],[57]. It is therefore
414 reasonable to assume that SPC can be used to remediate Cu, Co, Ni and/or Sb contaminated
415 soils by reducing the leachability of heavy metals and improving the soil strength. Further
416 studies of the effectiveness of SPC binder in stabilizing Cu, Co, Ni and/or Sb contaminated
417 soils are warranted. In addition, due to the significantly reduced metal leachability and
418 strengthened mechanical properties, it is supposed that the SPC stabilized soils can be reused
419 in a wide range of applications, e.g., roadway subgrade material, which need investigations in
420 further studies. This study deals with laboratory-scale tests, whereas future field trials should
421 be carried out to evaluate the effectiveness of SPC in stabilizing contaminated site soils.
422
423 **5 Conclusions**
424 In this study, SPC is utilized as a binder to solidify and stabilize a Pb, Zn and Cd
425 contaminated industrial site soil. The soil pH, TCLP and UCS tests are performed to evaluate
426 the effects of SPC content and curing time on the leachability and strength properties of the
427 contaminated soil. The mechanisms responsible for these changes in Pb, Zn, Cd leachability
428 and strength properties are evaluated by BCR SEP, SEM, XRD and MIP tests. Following can
429 be drawn based on the results obtained:
430 (1) Addition of SPC to contaminated soil changes the soil pH from acid to slightly
431 alkaline. High SPC content and long curing time result in high soil pH value.
432 (2) After SPC stabilization, the strength of the contaminated site soil is effectively
433 improved with increasing SPC content and curing time. The improvement is more significant
434 during the beginning 7 days of curing.
435 (3) SPC addition can significantly reduce the heavy metals leachability which is
436 substantiated by the TCLP test results. Depending on the curing time and SPC content, the
437 leached Pb, Zn and Cd concentrations can satisfy the corresponding TCLP and GB

5085.3-2007 regulatory limits.

(4) In the SEP tests, SPC addition is found to significantly reduce the acid soluble fractions while increasing residue fractions of Pb, Zn and Cd. The total pore volume of the soil is significantly reduced after SPC stabilization, and the reduction extent is dependent on the SPC content due to the pore filling effect of various reaction products.

(5) The XRD and SEM analyses reveal the formations of heavy-metal hydroxyapatites including $Pb_{10}(PO_4)_6(OH)_2$ and $Cd_5(PO_4)_3OH$) and phosphate-based precipitates including $Zn_3(PO_4)_2 \cdot 4H_2O$, $CaZn_2(PO_4)_2 \cdot 2H_2O$, $Pb_3(PO_4)$, $Cd_5H_2(PO_4)_4 \cdot 4H_2O$ and $(Cd_{0.65}Zn_{2.35})(PO_4)_2$ are the primary mechanisms for immobilizing Cd, Pb and Zn in the contaminated soil.

Acknowledgements

The authors appreciate the support of Environmental Protection Scientific Research Project of Jiangsu Province [Grant No. 2016031], National High Technology Research and Development Program of China [Grant No. 2013AA06A206], and National Natural Science Foundation of China [Grant No. 41330641 and 41472258].

References

[1] Du YJ, Jiang NJ, Liu SY, Jin F, Singh DN, Puppala AJ. Engineering properties and microstructural characteristics of cement-stabilized zinc-contaminated kaolin. Can Geotech J 2013; 51(3): 289-302. DOI: 10.1139/cgj-2013-0177

[2] Chen YM, Wang YZ, Xie HJ, Jiang YS. Adsorption characteristics of loess-modified natural silt towards pb(II): equilibrium and kinetic tests. Chin J Geotech Eng 2014; 36(7): 1185-1194. DOI: 10.11779/CJGE201407001

[3] Li HZ, Hu LM, Song DJ, Lin F. Characteristics of micro-nano bubbles and potential application in groundwater bioremediation. Water Environ Res 2014; 86(9): 844-851.

463 DOI: 10.2175/106143014X14062131177953
464 [4] MEP of PRC. Report on the national general survey on soil contamination. Ministry of
465 Environmental Protection of the People's Republic of China (MEP of PRC), Beijing.
466 2014:1-5.
467 [5] Singh TS, Pant KK. Solidification/stabilization of arsenic containing solid wastes using
468 portland cement, fly ash and polymeric materials. J Hazard Mater 2006; 131(1): 29-36.
469 DOI: 10.1016/j.jhazmat.2005.06.046
470 [6] Arulrajah A, Mohammadinia A, D'Amico A, Horpibulsuk S. Cement kiln dust and fly ash
471 blends as an alternative binder for the stabilization of demolition aggregates. Constr
472 Build Mater 2017;145: 218-225. DOI: 10.1016/j.conbuildmat.2017.04.007
473 [7] Hoy M, Rachan R, Horpibulsuk S, Arulrajah A, Mirzababaei M. Effect of wetting–drying
474 cycles on compressive strength and microstructure of recycled asphalt pavement–Fly ash
475 geopolymer. Constr Build Mater 2017; 144: 624-634. DOI:
476 10.1016/j.conbuildmat.2017.03.243
477 [8] Koutsopoulos S. Synthesis and characterization of hydroxyapatite crystals: a review
478 study on the analytical methods. J Biomed Mater Res 2002; 62(4): 600-612. DOI:
479 10.1002/jbm.10280
480 [9] Dai H, Lu X, Peng Y, Zou H, Shi J. An efficient approach for phosphorus recovery from
481 wastewater using series-coupled air-agitated crystallization reactors. Chemosphere 2016,
482 165: 211-220. DOI: 10.1016/j.chemosphere.2016.09.001
483 [10] Zhu R, Yu R, Yao J, Mao D, Xing C, Wang D. Removal of Cd^{2+} from aqueous solutions
484 by hydroxyapatite. Catal Today 2008; 139(1): 94-99. DOI: 10.1016/j.cattod.2008.08.011
485 [11] Liu Y, Yan YB, Seshadri B, Qi FJ, Xu YL, Bolan N, Zheng FL, Sun XY, Han WQ, Wang
486 LJ. Immobilization of lead and copper in aqueous solution and soil using hydroxyapatite
487 derived from flue gas desulphurization gypsum. J Geochem Expl 2016.

DOI:10.1016/j.gexplo.2016.08.006.

[12] Corami A, Mignardi S, Ferrini V. Cadmium removal from single-and multi-metal (Cd+Pb+Zn+Cu) solutions by sorption on hydroxyapatite. J Colloid Interface Sci 2008; 317(2): 402-408. DOI: 10.1016/j.jcis.2007.09.075

[13] Mavropoulos E, Rossi AM, Costa AM, Perez CAC, Moreira JC, Saldanha M. Studies on the mechanisms of lead immobilization by hydroxyapatite. Environ Sci Technol 2002; 36(7): 1625-1629. DOI: 10.1021/es0155938

[14] Miyaji F, Kono Y, Suyama Y. Formation and structure of zinc-substituted calcium hydroxyapatite. Mater Res Bull 2005; 40(2): 209-220. DOI: 10.1016/j.materresbull.2004.10.020

[15] Xu Y, Schwartz FW, Traina SJ. Sorption of Zn^{2+} and Cd^{2+} on hydroxyapatite surfaces. Environ Sci Technol 1994; 28(8): 1472-1480. DOI: 10.1021/es00057a015

[16] Xu Y, Schwartz FW. Lead immobilization by hydroxyapatite in aqueous solutions. J Contam Hydrol 1994; 15(3): 187-206. DOI: 10.1016/0169-7722(94)90024-8

[17] Ryan JA, Zhang P, Hesterberg D, Chou J, Sayers DE. (Formation of chloropyromorphite in a lead-contaminated soil amended with hydroxyapatite. Environ Sci Technol 2001; 35(18): 3798-3803. DOI: 10.1021/es010634l

[18] Boisson J, Ruttens A, Mench M, Vangronsveld, J.. Evaluation of hydroxyapatite as a metal immobilizing soil additive for the remediation of polluted soils. Part 1. Influence of hydroxyapatite on metal exchangeability in soil, plant growth and plant metal accumulation[J]. Environ Pollut 1999; 104(2): 225-233. DOI: 10.1016/S0269-7491(98)00184-5

[19] Monmaturapoj N. Nano-size hydroxyapatite powders preparation by wet-chemical precipitation route. J Met Mate Miner 2008; 18(1): 15-20.

[20] Serraj S, Boudeville P, Terol A. Effect of mechanical grinding of MCPM and CaO

513 mixtures on their composition and on the mechanical properties of the resulting
514 self-setting hydraulic calcium phosphate cements. J Mater Sci Mater Med 2001; 12(1):
515 45-50. DOI: 10.1023/A:1013805118391
516 [21] Boudeville P, Serraj S, Leloup JM, Margerit J, Pauvert B, Terol A. Physical properties
517 and self-setting mechanism of calcium phosphate cements from calcium
518 bis-dihydrogenophosphate monohydrate and calcium oxide. J Mater Sci Mater Med
519 1999; 10(2): 99-109. DOI: 10.1023/A:1008921104080
520 [22] Ginebra MP, Traykova T, Planell JA. Calcium phosphate cements as bone drug delivery
521 systems: a review. J Control Release 2006; 113(2): 102-110. DOI:
522 10.1016/j.jconrel.2006.04.007
523 [23] Wang XH, Ma JB, Wang YN, He BL. Reinforcement of calcium phosphate cements with
524 phosphorylated chitin. Chin J Polym Sci 2002; 20(4): 325-332. DOI:
525 10.3321/j.issn:0256-7679.2002.04.005
526 [24] Crannell BS, Eighmy TT, Krzanowski JE, Eusden JD, Shaw EL, Francis CA. Heavy
527 metal stabilization in municipal solid waste combustion bottom ash using soluble
528 phosphate. Waste Manage 2002; 20(2): 135-148. DOI:
529 10.1016/S0956-053X(99)00312-8
530 [25] Matusik J, Bajda T, Manecki M. Immobilization of aqueous cadmium by addition of
531 phosphates. J Hazard Mater 2008; 152(3): 1332-1339. DOI:
532 10.1016/j.jhazmat.2007.08.010
533 [26] ASTM standard D4318. Standard test methods for liquid limit, plastic limit, and
534 plasticityindex of soils. American Society for Testing and Materials (ASTM), West
535 Conshohocken, Pa. 2010.
536 [27] ASTM standard D2487. Standard practice for classification of soils for engineering
537 purposes (Unified Soil Classification System). American Society for Testing and

538 Materials (ASTM), West Conshohocken, Pa. 2011.
539 [28] Hernandez L, Probst A, Probst JL, Ulrich E. Heavy metal distribution in some French
540 forest soils: evidence for atmospheric contamination. Sci Total Environ 2003; 312(1):
541 195-219. DOI: 10.1016/S0048-9697(03)00223-7
542 [29] Arulrajah A, Kua T A, Horpibulsuk S, Phetchuay C, Suksiripattanapong C, Du YJ.
543 Strength and microstructure evaluation of recycled glass-fly ash geopolymer as
544 low-carbon masonry units. Constr Build Mater 2016; 114: 400-406. DOI:
545 10.1016/j.conbuildmat.2016.03.123
546 [30] Nan Z, Li J, Zhang J, Cheng G. Cadmium and zinc interactions and their transfer in
547 soil-crop system under actual field conditions. Sci Total Environ 2002; 285(1), 187-195.
548 DOI: 10.1016/S0048-9697(01)00919-6
549 [31] Du YJ, Wei ML, Reddy KR, Wu HL. Effect of carbonation on leachability, strength and
550 microstructural characteristics of KMP binder stabilized Zn and Pb contaminated soils.
551 Chemosphere 2016; 144: 1033-1042. DOI: 10.1016/j.chemosphere.2015.09.082
552 [32] ASTM standard D4219. Standard test method for unconfined compressive strength index
553 of chemical-grouted soils. American Society for Testing and Materials (ASTM), West
554 Conshohocken, Pa. 2008
555 [33] ASTM standard D4972. Standard test method for pH of soils. American Society for
556 Testing and Materials (ASTM), West Conshohocken, Pa. 2001
557 [34] USEPA Method 1311. Toxicity Characteristic Leaching Procedure (TCLP). United States
558 Environmental Protection Agency (USEPA), Washington, DC. 1992
559 [35] Rauret G, López-Sánchez JF, Sahuquillo A, Rubio R, Davidson C, Ure A, Quevauviller P.
560 Improvement of the BCR three step sequential extraction procedure prior to the
561 certification of new sediment and soil reference materials. J Environ Monit 1999; 1(1):
562 57-61. DOI: 10.1039/A807854H

563 [36] Horpibulsuk S, Rachan R, Raksachon Y. Role of fly ash on strength and microstructure
564 development in blended cement stabilized silty clay. Soils Found 2009; 49(1): 85-98.
565 DOI: 10.3208/sandf.49.85
566 [37] Jin F, Wang F, Al-Tabbaa A. Three-year performance of in-situ solidified/stabilised soil
567 using novel MgO-bearing binders. Chemosphere 2016;144: 681-688. DOI:
568 10.1016/j.chemosphere.2015.09.046
569 [38] Horpibulsuk S, Rachan R, Chinkulkijniwat A, Raksachon Y, Suddeepong A. Analysis of
570 strength development in cement-stabilized silty clay from microstructural considerations.
571 Constr Build Mater 2010; 24(10): 2011-2021. DOI: 10.1016/j.conbuildmat.2010.03.011
572 [39] Sasanian S, Newson TA. Use of mercury intrusion porosimetry for microstructural
573 investigation of reconstituted clays at high water contents. Eng Geol 2013; 158: 15-22.
574 DOI: 10.1016/j.enggeo.2013.03.002
575 [40] Jiang NJ, Du YJ, Liu SY, Wei ML, Horpibulsuk S, Arulrajah A. Multi-scale laboratory
576 evaluation of the physical, mechanical, and microstructural properties of soft highway
577 subgrade soil stabilized with calcium carbide residue. Canadian Can Geotech J 2015;
578 53(3): 373-383. DOI: 10.1139/cgj-2015-0245
579 [41] Earl JS, Wood DJ, Milne SJ. Hydrothermal synthesis of hydroxyapatite. Phys: Conf Ser
580 2006; 26(1): 268-271. DOI:10.1088/1742-6596/26/1/064
581 [42] Arsad MSM, Lee PM, Hung LK. Synthesis and characterization of hydroxyapatite
582 nanoparticles and β-TCP particles. 2nd International Conference on Biotechnology and
583 Food Science 2011; 7: 184-188.
584 [43] Mavropoulos E, Rocha NC, Moreira JC, Rossi AM, Soares GA. Characterization of
585 phase evolution during lead immobilization by synthetic hydroxyapatite. Mater Charact
586 2004; 53(1): 71–78. DOI: 10.1016/j.matchar.2004.08.002
587 [44] Liang W, Zhan L, Piao L, Rüssel C. Lead and copper removal from aqueous solutions by

porous glass derived calcium hydroxyapatite. Mater Sci Eng B 2011; 176: 1010–1014. DOI: 10.1016/j.mseb.2011.05.036

[45] Du YJ, Wei ML, Reddy KR, Jin F, Wu HL, Liu ZB. New phosphate-based binder for stabilization of soils contaminated with heavy metals: Leaching, strength and microstructure characterization. J Environ Manag 2014; 146: 179-188. DOI: 10.1016/j.jenvman.2014.07.035

[46] Mignardi S, Corami A, Ferrini V. Evaluation of the effectiveness of phosphate treatment for the remediation of mine waste soils contaminated with Cd, Cu, Pb, and Zn. Chemosphere 2012; 86(4): 354-360. DOI: 10.1016/j.chemosphere.2011.09.050

[47] Oliva J, De Pablo J, Cortina JL, Cama J, Ayora C. Removal of cadmium, copper, nickel, cobalt and mercury from water by Apatite II™: Column experiments. J Hazard Mater 2011; 194: 312-323. DOI: 10.1016/j.jhazmat.2011.07.104

[48] Dong LJ, Zhu ZL, Qiu YL, Zhao JF. Advance in Research of Heavy Metals Removal by Hydroxyapatite and its Composite. Chemistry 2013; 76 (5): 405-410. DOI: 10.14159/j.cnki.0441-3776.2013.05.015

[49] Luo J, Chen J, Li W, Huang Z, Chen C. Temperature Effect on Hydroxyapatite Preparation by Co-precipitation Method under Carbamide Influence. MATEC Web of Conferences 2015, 26: 01007. DOI: 10.1051/matecconf/20152601007

[50] Roeselers G, Van Loosdrecht MCM. Microbial phytase-induced calcium-phosphate precipitation—a potential soil stabilization method. Folia Microbiol 2010; 55(6): 621-624. DOI: 10.1007/s12223-010-0099-1

[51] Horpibulsuk S, Miura N, Nagaraj TS. Assessment of strength development in cement-admixed high water content clays with Abrams' law as a basis. Geotechnique 2003; 53(4): 439-444. DOI: 10.1680/geot.2003.53.4.439

[52] Ismail MA, Joer HA, Randolph MF, Meritt A. Cementation of porous materials using

calcite. Geotechnique 2002; 52(5): 313-324. DOI: 10.1680/geot.2002.52.5.313

[53] Du YJ, Wei ML, Reddy KR, Liu ZP, Jin F. Effect of acid rain pH on leaching behavior of cement stabilized lead-contaminated soil. J Hazard Mater 2014; 271:131-140. DOI: 10.1016/j.jhazmat.2014.02.002

[54] Kazi TG, Jamali MK, Kazi GH, Arain MB, Afridi HI, Siddiqui A. Evaluating the mobility of toxic metals in untreated industrial wastewater sludge using a BCR sequential extraction procedure and a leaching test. Anal Bioanal Chem 2005; 383(2): 297-304. DOI: 10.1007/s00216-005-0004-y

[55] Tokalıoğlu Ş, Kartal Ş. Multivariate analysis of the data and speciation of heavy metals in street dust samples from the Organized Industrial District in Kayseri (Turkey). Atmos Environ 2006; 40(16): 2797-2805. DOI: 10.1016/j.atmosenv.2006.01.019

[56] Gupta N, Kushwaha AK, Chattopadhyaya MC. Adsorptive removal of Pb^{2+}, Co^{2+} and Ni^{2+} by hydroxyapatite/chitosan composite from aqueous solution. J Taiwan Inst Chem Eng 2012; 43(1): 125-131. DOI: 10.1016/j.jtice.2011.07.009

[57] Ogawa S, Katoh M, Numako C, Kitahara K, Miyazaki S, Sato T. Immobilization of antimony (III) in oxic soil using combined application of hydroxyapatite and ferrihydrite. Water Air Soil Pollut 2016; 227(4): 124. DOI: 10.1007/s11270-016-2826-y

Table Captions

Table 1 Main physicochemical properties of contaminated soil used in the study

Table 2 Main chemical composition of SSP and CaO used in the study

Table 3 Basic properties of samples used for different tests

Figure Captions

Figure 1 pH variation of the SPC stabilized soil at different curing times

Figure 2 Development of unconfined compressive strength of the stabilized soil at different curing times

Figure 3 TCLP leached heavy metal concentrations of the stabilized soil at different curing times: (a) Pb; (b) Zn; and (c) Cd

Figure 4 SEP test results of the SPC stabilized soil after 28 days of curing: (a) Zn; (b) Pb; and (c) Cd

Figure 5 MIP test results for SPC stabilized soil cured for 28 days: (a) pore size distribution, and (b) volumes of different types of pores

Figure 6 X-ray diffractograms of the samples cured for 28 days: (a) SPC paste; (b) SPC paste with 3% Pb; (c) SPC paste with 3% Zn; (d) SPC paste with 3% Cd; and (e) 8% SPC stabilized soil

Figure 7 SEM images of samples cured for 28 days: (a) SPC paste; (b) SPC paste with 3% Pb; (c) SPC paste with 3% Zn; (d) SPC paste with 3% Cd; and (e) 8% SPC stabilized soil

663 **Table 1** Main physicochemical properties of contaminated soil used in the study

Index	Value
Plastic limit, w_P (%)[a]	17.2
Liquid limit, w_L (%)[a]	33.3
Soil type[b]	CL
Specific gravity, G_s	2.73
Organic matter (%)[c]	3.19
Heavy metal concentration (mg/kg)[d]	
Zinc (Zn)	17300
Lead (Pb)	9710
Cadmium (Cd)	2425
Grain size distribution (%)[e]	
Clay (<0.005 mm)	6.54
Silt (0.005 - 0.075 mm)	43.95
Sand (0.075-1 mm)	49.51

664 [a]Tests are performed as per ASTM D4318 [26].

665 [b]Based on the Unified Soil Classification System (USCS) [27].

666 [c]Organic matter is determined by loss on ignition.

667 [d]Complete dissolution of samples is performed by acid digestion method using a mixture of

668 $HF/HNO_3/HClO_4/H_2O_2$ [28].

669 [e]Measured using a laser particle size analyzer Master-sizer 2000.

670

671

672

673

674

675

676

677

678

679

680

Table 2 Main chemical composition of SSP and CaO used in the study

Parameter	SSP[a]	CaO[b]
CaO (%)	ND[c]	98.9
H_3PO_4 (%)	2.6	ND[c]
Available P_2O_5 (%)	14.5	ND[c]
Cl (%)	0.003	0.002
SO_4 (%)	0.002	0.04
Pb (%)	0.0015	0.002
MgO (%)	0.05	0.2
Fe (%)	0.005	0.013
As (%)	0.0005	ND[c]
NH_4 (%)	0.011	0.015
NO_3 (%)	0.001	ND[c]

[a] Data obtained from the Sinopharm Chemical Reagent Co. Ltd.

[b] Data obtained from the Nanjing Chemical Reagent Co. Ltd.

[c]Note: "ND" means not determined.

700 **Table 3.** Basic properties of samples used for different tests

Test type	SPC content (%)	Curing time (days)	Number of identical samples
Soil pH	0[a], 4, 6, 8, 10	7, 14, 28	3
UCS	0[a], 4, 6, 8, 10	7, 14, 28	3
TCLP	0[a], 4, 6, 8, 10	7, 14, 28	3
SEP	0[a], 4, 8	28	1
MIP	4, 6, 8, 10	28	1
XRD	8, SPC pastes[b]	28	1
SEM	8, SPC pastes[b]	28	1

701 [a]0% SPC content means untreated soil

702 [b]SPC pastes include SPC paste, SPC paste with 3% Pb, SPC paste with 3% Zn, and SPC

703 paste with 3% Cd

704

705

706

707

708

709

710

711

712

713

714

715

716

717

718

719

720